the plant journal

SEB SOCIETY FOR EXPERIMENTAL BIOLOGY

The Plant Journal (2020) **103,** 1575–1589 doi: 10.1111/tpj.14848

AKR2A interacts with KCS1 to improve VLCFAs contents and chilling tolerance of *Arabidopsis thaliana*

Lin Chen[1], Wenjun Hu[1], Neelam Mishra[2], Jia Wei[1], Hongling Lu[1], Yuqi Hou[4], Xiaoyun Qiu[1], Shaofang Yu[1], Changlu Wang[4], Hong Zhang[3], Yifan Cai[3], Chunyan Sun[4] and Guoxin Shen[1,*]

[1]*State Key Laboratory for Quality and Safety of Agro-products, Zhejiang Academy of Agricultural Sciences, Hangzhou 310021, China,*

[2]*Department of Botany St Joseph's College (Autonomous), Bengaluru 560027, India,*

[3]*Department of Biological Sciences, Texas Tech University, Lubbock, TX 79409, USA, and*

[4]*Tianjin University of Science & Technology, Hexi District, Tianjin 300457, China*

Received 26 April 2019; revised 28 April 2020; accepted 5 May 2020; published online 20 May 2020.
*For correspondence (e-mail guoxin.shen@ttu.edu).

SUMMARY

Arabidopsis thaliana **AKR2A plays an important role in plant responses to cold stress. However, its exact function in plant resistance to cold stress remains unclear. In the present study, we found that the contents of very long-chain fatty acids (VLCFAs) in *akr2a* mutants were decreased, and the expression level of KCS1 was also reduced. Overexpression of *KCS1* in the *akr2a* mutants could enhance VLCFAs contents and chilling tolerance. Yeast-2-hybrid and bimolecular fluorescence complementation (BIFC) results showed that the transmembrane motif of KCS1 interacts with the PEST motif of AKR2A both *in vitro* and *in vivo*. Overexpression of *KCS1* in *akr2a* mutants rescued *akr2a* mutant phenotypes, including chilling sensitivity and a decrease of VLCFAs contents. Moreover, the transgenic plants co-overexpressing *AKR2A* and *KCS1* exhibited a greater chilling tolerance than the plants overexpressing *AKR2A* or *KCS1* alone, as well as the wild-type. *AKR2A* knockdown and *kcs1* knockout mutants showed the worst performance under chilling conditions. These results indicate that AKR2A is involved in chilling tolerance via an interaction with KCS1 to affect VLCFA biosynthesis in *Arabidopsis*.**

Keywords: AKR2A, KCS1, very long-chain fatty acids, chilling tolerance.

INTRODUCTION

Low temperature is an important environmental factor limiting the geographical distribution and productivity of plants (Saibo *et al.*, 2009; Chinnusamy *et al.*, 2010). To cope up with cold stress, plants have evolved several physiological and molecular adaptations that reduce the cold-induced damage; these adaptations include the reduction or cessation of growth, changes in membrane composition, the enhanced activity of antioxidant enzymes, the rapid expression of low-temperature-related genes, and increased levels of compatible osmolytes (Graham and Patterson, 1982; Williams *et al.*, 1992). High levels of unsaturated fatty acids in the membrane lipids are closely associated with a plant's tolerance to low temperatures (Palta *et al.*, 1993).The effects of polyunsaturated fatty acids, such as C18:2 or C18:3, on the recovery of membrane fluidity under low temperatures have long been established (Chen and Thelen, 2013). However, the role of very long-chain fatty acids (VLCFAs), which have more than 20 carbons in their carbon chains, in cold tolerance remains unclear.

The VLCFAs incorporated into plant lipids are derived from the iterative addition of C2 units provided by malonyl-CoA to an acyl-CoA by the 3-ketoacyl-CoA synthase (KCS) component of a fatty acid elongase complex (Millar and Kunst, 1997; Bach *et al.*, 2008; Joubes *et al.*, 2008; Nobusawa and Umeda, 2012). In plants, KCS enzymes are encoded by a gene family that consists of 21 members in *Arabidopsis thaliana*. The lengths of the fatty acid chains incorporated into seed triacylglycerols depending upon the substrate specificity of the KCS. KCS1 encodes a 3-ketoacyl-CoA synthase that is involved in VLCFA synthesis in vegetative tissues, and plays a role in wax biosynthesis (Todd *et al.*, 1999; Smirnova *et al.*, 2013). The deletion of *KCS1* resulted in the loss of up to 80% of C26 to C30 wax alcohols and aldehydes. The expression of *KCS1* in *Saccharomyces cerevisiae* cells demonstrated that KCS1 plays an important role in the synthesis of C20:0, C20:1, and C22:0 (Tresch *et al.*, 2012). The expression levels of all KCS genes were affected by cold treatment, and the expression of *KCS1* was significantly reduced under chilling stress (Todd *et al.*, 1999).

Arabidopsis thaliana Ankyrin Repeat-containing protein (AKR2A) is a molecular chaperone that binds to the transmembrane domains of interacting proteins to prevent its aggregation and direct them to the right location after translation (Hong *et al.*, 2010; Shen *et al.*, 2010). Three akr2a point mutations, S25F (T1, Ser-to-Phe change at residue 25), P113L (T3, Pro-to-Leu change at residue 113), and E150K (T6, Glu-to-Lys change at residue 150), give rise to similar phenotypes. These *akr2a* mutants also displayed increased sensitivity to chilling conditions, which demonstrates that AKR2A plays various important roles in plant cellular metabolism and is essential for plant growth and development (Shen *et al.*, 2010). An analysis of the fatty acid composition of *akr2a* mutants showed that their VLCFAs contents were lower than that of the wild-type Col er105 (BM), indicating that AKR2A plays an important role in the synthesis of VLCFAs and affects the extent of a plant's chilling tolerance. Our results showed that AKR2A interacted with KCS1, and also that overexpression of *KCS1* in *akr2a* mutant could enhance the plant chilling tolerance and VLCFA levels, suggesting that AKR2A mediates VLCFA synthesis and affects the chilling tolerance capability in Arabidopsis.

RESULTS

The expression of *AKR2A* increased under chilling condition

To investigate the expression pattern of AKR2A under chilling conditions, a transgenic line was generated where the *AKR2A* promoter sequence was fused to the gene for GUS (Figure 1a). The *AKR2A* promoter activity was visualized via histochemical staining for GUS using 14-day-old seedlings, leaves from 4-week-old plants, flowers, and three different stages of siliques (Siliques I, 2 days after flowering; Siliques II, 5 days after flowering; Siliques II, 10 days after flowering). We analyzed GUS expression in 14-day-old seedlings, the leaves of 3-week-old plants, flowers and siliques. Deeper GUS staining was detected in the chilling-treated transgenic plants compared to that in normal conditions, indicating that the expression of *AKR2A* was increased under chilling conditions (Figure 1b). Real-time polymerase chain reaction (PCR) assays were performed to detect the *AKR2A* expression under normal and chilling conditions. Total RNA was isolated from 14-day-old seedlings, leaves from 4-week-old plants, flowers, and siliques in three different developmental stages. Consistent with the GUS staining results, the real-time PCR analysis showed increased *AKR2A* expression under chilling conditions (Figure 1c). These results indicate that *AKR2A* responded to chilling stress.

Proteins interact with AKR2A in a yeast-2-hybrid system

As shown in Figure 1 AKR2A participated in the chilling stress response. To further determine the function of AKR2A in chilling, a yeast-2-hybrid assay was performed to identify the proteins that interact with AKR2A. Consequently, 133 proteins were characterized and 95 (71%) of these were transmembrane proteins (Figure 2a). Further analysis showed that 10 proteins were involved in fatty acid biosynthesis. Thus, AKR2A may affect a plant's chilling stress response by mediating fatty acid synthesis (Figure 2b).

AKR2A interacts with the transmembrane domain of KCS1

The yeast-2-hybrid assay showed that AKR2A interacted with KCS1, an important protein that participates in the biosynthesis of VLCFAs. The yeast-2-hybrid assay was performed to determine the domains involved in AKR2A–KCS1 binding. Previous studies have found that the PEST domain of AKR2A specifically interacts with the transmembrane residues of interacting proteins (Shen *et al.*, 2010). An AKR2A binding sequence (transmembrane motif with more than one positive amino acid residues in a 10 amino acid flanking sequence) was detected in KCS1. This observation suggested that AKR2A could interact with KCS1. To determine whether the PEST domain in AKR2A binds KCS1, residues 1–207 of AKR2A were divided into two parts: one possessing the PEST domain (residues 1–40 of AKR2A) and the other containing the remaining residues (41–207 of AKR2A) (Figure 2c). Full-length KCS1 and three KCS1 deletion fragments were also constructed. The results clearly show that the AKR2A binding site in KCS1 is the transmembrane domain (residues 40–80 of KCS1), whereas the region in AKR2A involved in binding to KCS1 is the PEST domain (residues 1–40 of AKR2A). Our data agree with the previous results indicating that AKR2A binds to a transmembrane sequence.

The KCS enzyme is assumed to determine substrate and tissue specificities in fatty acid elongation (Fehling and Mukherjee, 1991). VLCFAs result from the elongation of C18 fatty acids by malonyl-CoA in the presence of NADH and NADPH (Nugteren, 1965; Jr and Sprecher, 1977; Jr and Sprecher, 1979). The Arabidopsis KCS family includes 21 members, with KCS1 being highly expressed in leaves and responsible for producing saturated and unsaturated VLCFAs with chains of up to 22 carbon atoms (Todd *et al.*, 1999; Tresch *et al.*, 2012).

Yeast-2-hybrid results showed that AKR2A interacted with the transmembrane motif of KCS1, comprising the ABS motif described previously. Thereafter, a bimolecular fluorescence complementation (BIFC) assay was performed to test whether the AKR2A–KCS1 interaction takes place *in vivo*. The results show that the PEST motif of AKR2A interacted with the transmembrane motif of KCS1 *in vivo* (Figure 2d).

KCS1 expression level and VLCFAs contents were reduced in *akr2a*-TILLING mutants

AKR2A is essential for development and growth of *Arabidopsis* and plays an important role in chilling

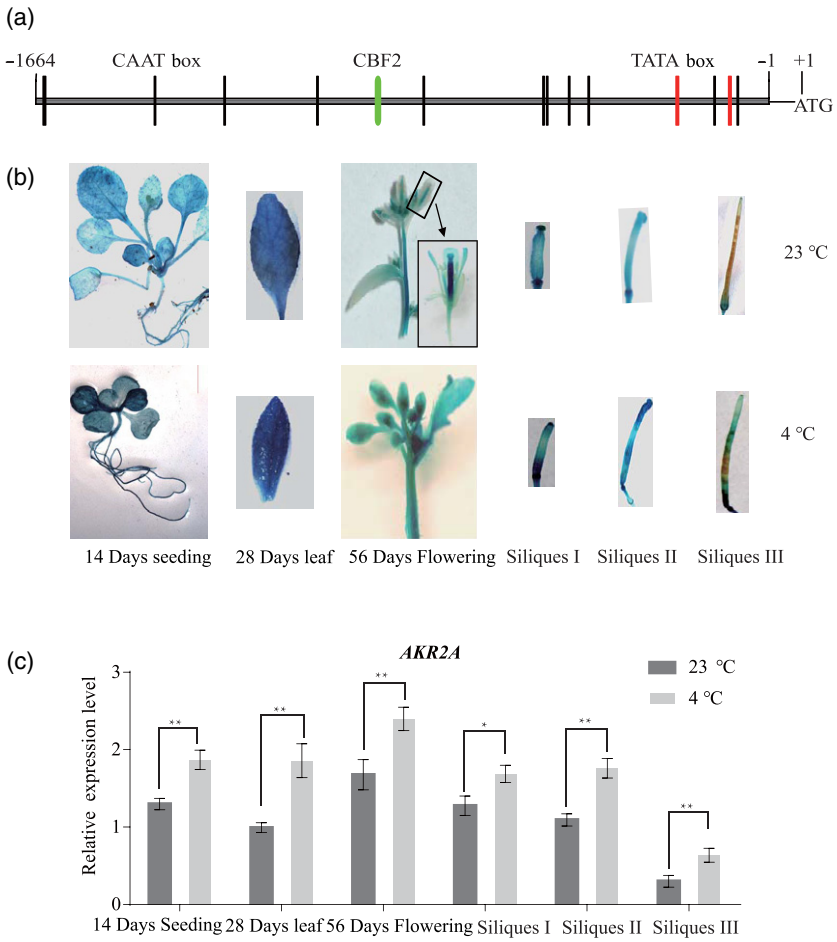

Figure 1. The expression of *AKR2A* increased under chilling conditions.
(a) Analysis of the *AKR2A* promoter sequence. The putative cis-elements (TATA boxes and CAAT boxes) are shownin the *AKR2A* promoter region [5′ region upstream from the start codon (ATG) of the *AKR2A* coding sequence]. Numbers indicate the positions relative to the translation start codon starting from the adenosine (A, +1). The putative TATA boxes are indicated in green and CAAT boxes are indicated in red. The putative CBF2 element is indicated by a blue box.
(b) Transgenic Arabidopsis harboring the *AKR2A* promoter fused to the gene for GUS were constructed and grown under normal or chilling conditions.
(c) Real-time polymerase chain reaction analysis of *AKR2A* expression. The wild-type genotype was grown under normal or chilling conditions. The relative transcript abundance of Actin8 was used to normalize for different amounts of the total RNA amount. The results show relative transcript abundance. The data represent the mean ± SD of three replicates.

tolerance. The AKR2A–KCS1 interaction suggested that AKR2A is involved in the process of VLCFA biosynthesis. Real-time PCR results showed that the transcriptional level of *KCS1* was not significantly affected in *akr2a*-TILLING mutants (Figure 3a). However, a western blot assay showed that the KCS1 expression level was reduced in *akr2a*-TILLING mutants. These results indicate that AKR2A affected KCS1 expression at the protein level (Figure 3b,c).

To determine the role of AKR2A in fatty acid metabolism, the fatty acid compositions of the wild-type and *akr2a*-TILLING mutants were analyzed. The most abundant fatty acids detected in the leaves were C16:0, C18:2, and C18:3. These three accounted for more than 90% of the total, and no differences were detected in the *akr2a*-TILLING mutants. The C16:1 and C18:1 levels were higher in *akr2a* mutants than in the wild-type. However, C14:0, C20:0, C20:3, C22:0, C24:0, and C22:6 levels were reduced in *akr2a* mutants. Total VLCFAs contents were significantly decreased in the *akr2a* mutants (Figure 3d). Therefore, VLCFAs biosynthesis could be affected by the *akr2a*-TILLING mutants.

The overexpression of *KCS1* enhanced the chilling tolerance of *akr2a* mutants

akr2a-TILLING mutants are sensitive to chilling. To determine whether this phenotype was caused by the *KCS1* reduction, *KCS1* was expressed under the 35S promoter in BM and *akr2a*-TILLING mutants (Figure 4a). For normal conditions, the seedlings were grown under 23°C for 24 days. For chilling tolerance assays, 10-day-old seedlings were treated with cold (4°C) for 14 days. To determine the expression level of KCS1 in the wild-type, the *akr2a* mutant, and the *KCS1*-overexpressing line, cell extracts

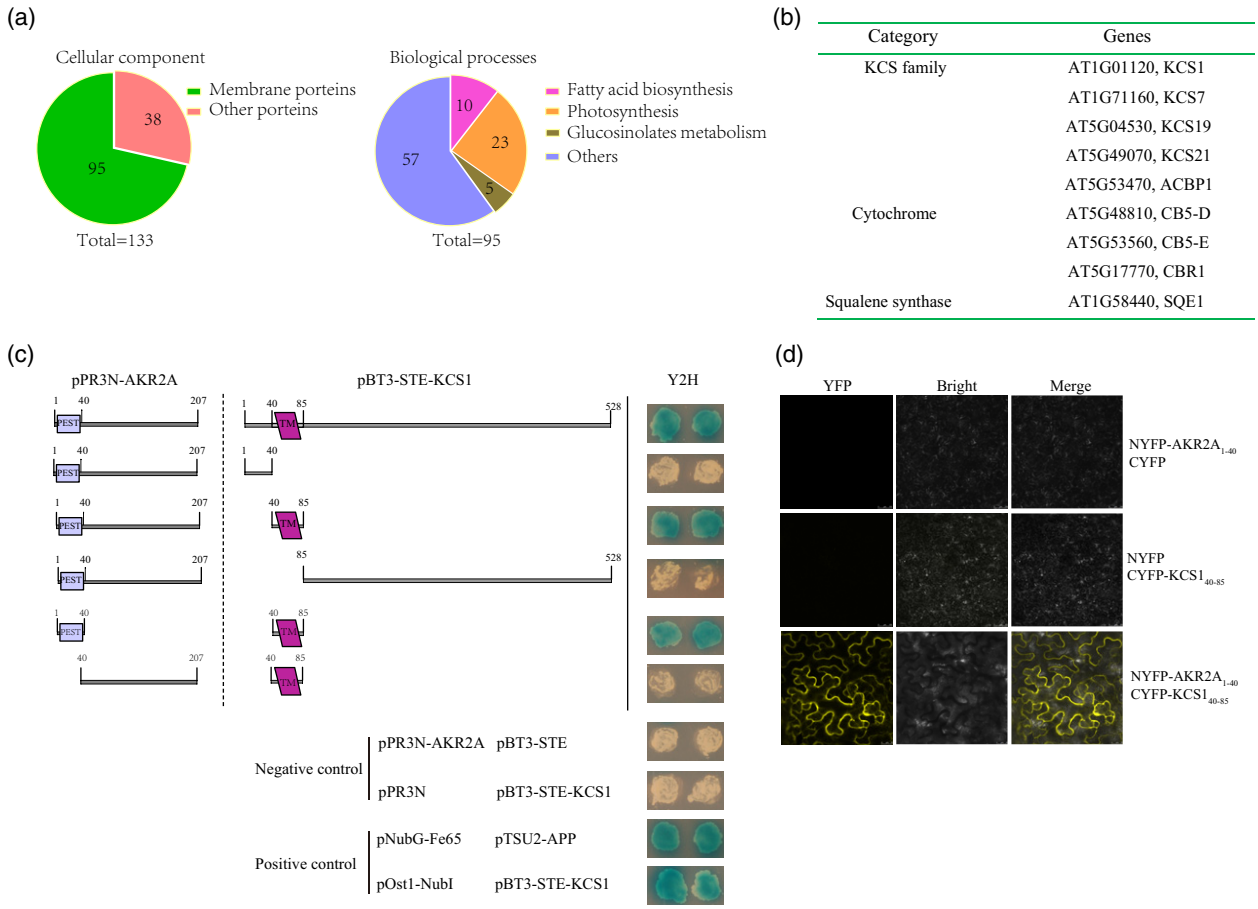

Figure 2. Identification of AKR2A interacting proteins by a yeast-2-hybrid assay.
(a) Yeast-2-hybrid screening and protein classification.
(b) Proteins participating in fatty acid metabolism are listed.
(c) Membrane based yeast-2-hybrid technique to identify the putative interactions domains of AKR2A and KCS1. (d) Bimolecular fluorescence complementation assay to confirm the interaction of AKR2A and KCS1 *in vivo* where the N-terminal of yellow fluorescent protein (YFP) is fused to AKR2A and the C-terminal of YFP is fused to KCS1.

from these plants were used for western blotting. The results show higher *KCS1* expression levels in BM-OK1, T1-OK1, T3-OK1, and T6-OK1 than in BM, T1, T3, and T6, respectively (Figure 4b).

There was essentially no phenotypic difference among BM, BM-OK1, T1, T1-OK1, T3, T3-OK1, T6, and T6-OK1 at 23°C, However, when grown at 6°C, reduced statures were observed for T1, T3, and T6. The *KCS1*-overexpressing line, BM-OK1, T1-OK1, T3-OK1, and T6-OK1, showed enhanced cold tolerance compared to BM, T1, T3, and T6 (Figure 4c,d), respectively. These observations suggested that the *akr2a* mutation affected plant growth under low temperature and that overexpression of *KCS1* could enhance chilling tolerance.

The overexpression of *KCS1* increased VLCFAs contents and photosynthetic efficiency under chilling conditions

To give a quantitative overview of the mutant phenotype and its association with fatty acids, the fatty acid compositions of BM, BM-OK1, T1, T1-OK1, T3, T3-OK1, T6, and T6-OK1 were measured. The total fatty acid contents in T1, T3, and T6 mutants leaves were lower than that in BM, including a lower content of C20:0, C22:0, and C24:0. However, the total fatty acid contents in T1-OK1, T3-OK1, and T6-OK1 were higher than T1, T3, and T6, respectively. The C20:0 and C22:0 levels were further increased in the *KCS1* overexpression lines (Figure 5a). Thus, our results were consistent with the previous study showing that KCS1 plays an important role in C20:0 and C22:0 synthesis and we concluded that total fatty acid contents were enhanced by the increased content of very long-chain fatty acids.

Because the overexpression mutants showed enhanced cold tolerance, we examined leaf electrolyte leakage under low temperature. Accordingly, 15-day-old plants were treated at 6°C for 14 days, and then the whole plants were excised for electrolyte leakage assays. T1, T3, and T6 showed higher levels of electrolyte leakage than BM at 6°C

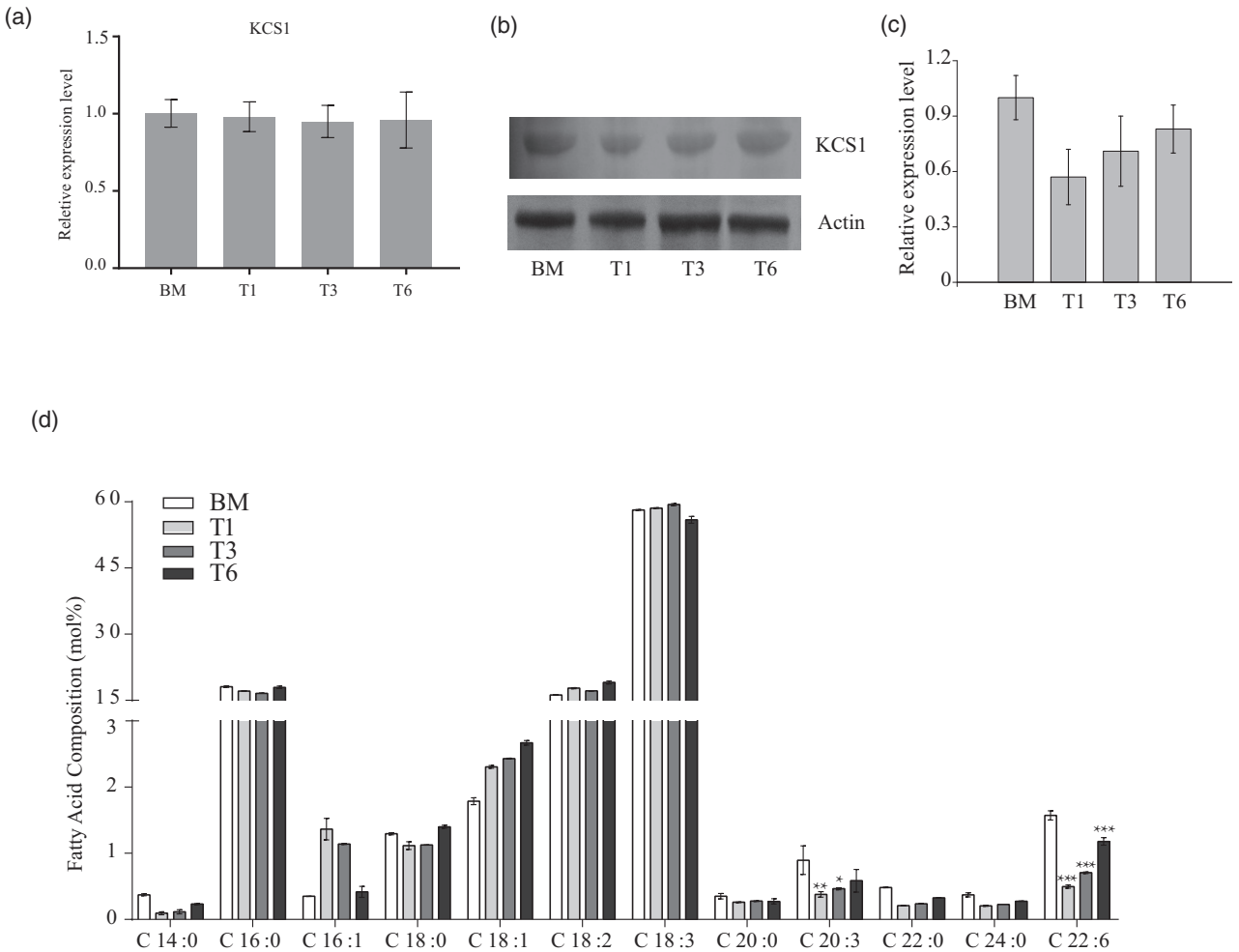

Figure 3. *KCS1* expression level and very long-chain fatty acid biosynthesis in *akr2a* mutants.
(a) The transcription analysis of *KCS1* by a quantitative polymerase chain reaction in the wild-type and *akr2a*-TILLING (T1, T3, and T6) mutants.
(b) The overall levels of KCS1were determined by immunoblotting using the protein extracts from the wild-type and T1, T3, and T6. Actin was used as a loading control.
(c) Analysis of the KCS1 expression level in (b).
(d) Analysis of the fatty acid composition of BM, T1, T3, and T6 leaves. Three biological replicates were performed. Error bars indicate the SD. Significance was determined using Student's *t*-test. $*P < 0.05$; $**P < 0.01$; $***P < 0.001$.

(Figure 5b). However, *KCS1* overexpression resulted in a similar decrease in electrolyte leakage. These results show that overexpression of *KCS1* in *akr2a* mutant plants is beneficial for maintaining the integrity of the plant cell.

The maximal photochemical efficiency of PS II (F_v/F_m) is a useful indicator for PS II damage in plants, and electrolyte leakage is commonly associated with the PSII damage. The F_v/F_m values for all plants were almost the same, indicating that the photochemical efficiency was not significantly affected under normal conditions. After 14 days of chilling, the F_v/F_m of BM decreased by 31.04%, whereas the F_v/F_m of BM-OK1 decreased by 27% (Figure 5c). The F_v/F_m value was higher in the *KCS1* overexpressing plants than in the *akr2a* mutant plants under chilling stress, suggesting that *KCS1* overexpression also enhances the photosynthetic efficiency.

After chilling treatment for 3 days, the *akr2a* mutants had less chlorophyll than wild-type plants (Figure S1a). Moreover, *KCS1* overexpression in *akr2a* mutants resulted in the higher chlorophyll content, indicating that overexpression of *KCS1* could partially inhibit the effects of the *akr2a* mutants on chilling-induced chlorophyll degradation.

The results for malondialdehyde (MDA) content, chlorophyll levels, anthocyanin contents, superoxide dismutase (SOD) activity, proline content, stomatal conductance, and transpiration rate showed that the chilling tolerance of BM-OK1, T1-OK1, T3-OK1, and T6-OK1 was increased compared to BM, T1, T3, and T6, separately, indicating that *KCS1* overexpression could increase a plant's chilling tolerance (Figure 5d, Figure S1, and Data S1). Investigation of the cold response genes *COR15A*, *DREB2A*, *KIN1*, and *RD29A* also showed that overexpression of *KCS1* enhances

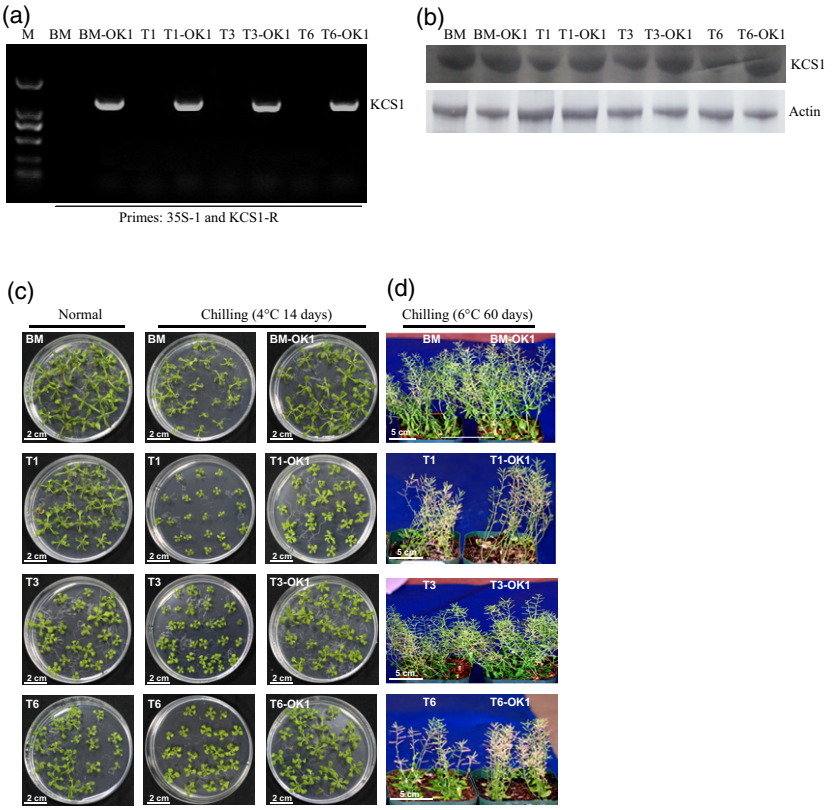

Figure 4. Overexpression of *KCS1* enhances the chilling tolerance of the *akr2a*-TILLING mutants.
(a) Polymerase chain reaction identification of the *KCS1* insertion in selected transgenic lines in a BM, T1, T3, and T6 background using primer pairs 35S and KCS1R.
(b) Western blot analysis of BM, *akr2a*-TILLING mutants and the corresponding overexpression *KCS1* line. An anti-KCS1 antibody was used to detect KCS1. Actin was used as the protein loading control.
(c) Representative photographs of BM, BM-OK1, T1, T1-OK1, T3, T3-OK1, T6, and T6-OK1 under cold stress. (d) BM, BM-OK1, T1, T1-OK1, T3, T3-OK1, T6, and T6-OK1 grown at 6°C for 60 days, then transferred to 4°C for 14 days.

the expression of these genes in wild-type and *akr2a* mutants under chilling conditions (Figure S2).

The overexpression of *KCS1* increased the expression levels of fatty acid biosynthesis related genes

Fatty acid analysis suggested that the expression of fatty acid genes in *akr2a* mutants was affected. Eight genes were selected to determine whether their expression patterns were affected. Real-time PCR results showed that the expression levels of fatty acid genes were decreased in *akr2a*-TILLING mutants and that *KCS1* overexpression could increase the expression levels of these genes (Figure 6).

The co-expression of *KCS1* and *AKR2A* increases chilling tolerance of Arabidopsis

To further determine functions of *KCS1* and *AKR2A* in chilling tolerance, *KCS1* and *AKR2A* were co-overexpressed in Arabidopsis (Figure 7a). The results of western blotting showed that the AKR2A expression level in Col-OA was higher than that in Col, and the *KCS1* expression level in OK1 was higher than that in Col (Figure 7b). KCS1 and AKR2A were both highly expressed in the *AKR2A* and *KCS1* co-expression line OA/OK1.

A chilling tolerance experiment was further performed to determine the chilling tolerance of OA, OK1, and OA/OK1. Both OA and OK1 showed greater chilling tolerance than Col (Figure 7c,d). However, OA/OK1 exhibited the highest chilling tolerance of all the four lines. Membrane leakage assay results were consistent with those of the chilling tolerance experiment. OA/OK1 showed the lowest membrane leakage under chilling stress, and the OA and OK1 plants also showed a significantly lower reduction than wild-type plants (Figure 8b). These results suggest that overexpressing *KCS1* and *AKR2A* could increase the chilling tolerance of *Arabidopsis*.

The co-overexpression of *KCS1* and *AKR2A* increased chilling tolerance and expression levels of fatty acid biosynthesis genes

The *akr2a* mutants showed reduced chilling tolerance and VLCFA synthesis, and transgenic plants overexpressing *AKR2A* (OA) enhanced the chilling tolerance of Arabidopsis (Figure 7d). VLCFAs contents in OA and OK1 were higher than that in wild-type, and OA/OK1 had the highest VLCFAs contents, with OA/OK1 showing the lowest levels of electrolyte leakage among the four lines (Figure 8a,b).

Consistent with the previous results, F_v/F_m is negatively correlated with membrane electrolytes. The wild-type Col had the highest membrane leakage among the four groups, and the F_v/F_m decreased by 32.06% after 14 days of chilling treatment. For OA and OK1, the F_v/F_m in Col decreased by 29.38% and 27.68%, respectively. However, the F_v/F_m of OA/OK1 decreased by only 25.93% (Figure 8c). The results

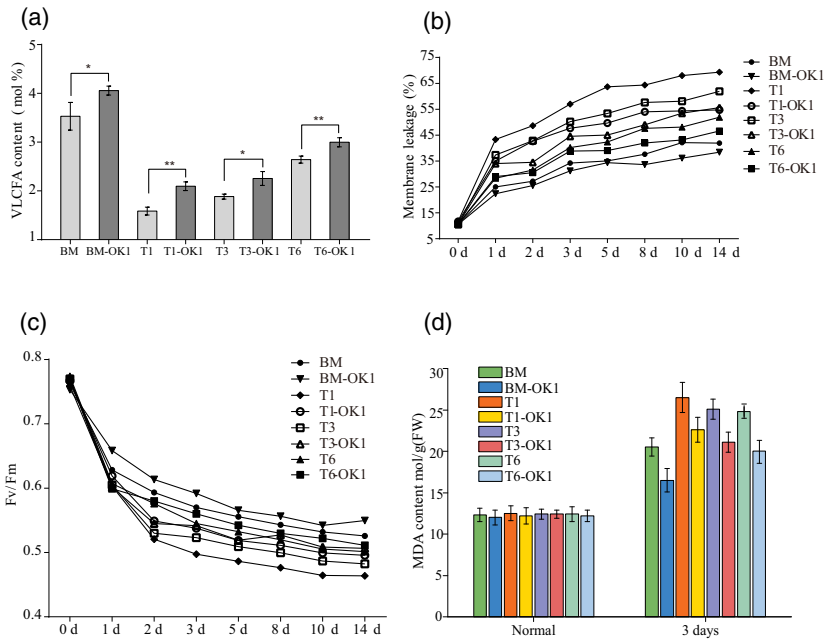

Figure 5. Overexpression of *KCS1* improves very long-chain fatty acids (VLCFAs) production and membrane stability.
(a) VLCFAs contents of BM, T1, T3, T6, and the corresponding *KCS1* overexpressing line.
(b) Membrane leakage in response to chilling stress
(c) Average F_v/F_m values in response to chilling stress.
(d) Malondialdehyde (MDA) content in plants in response to chilling conditions.

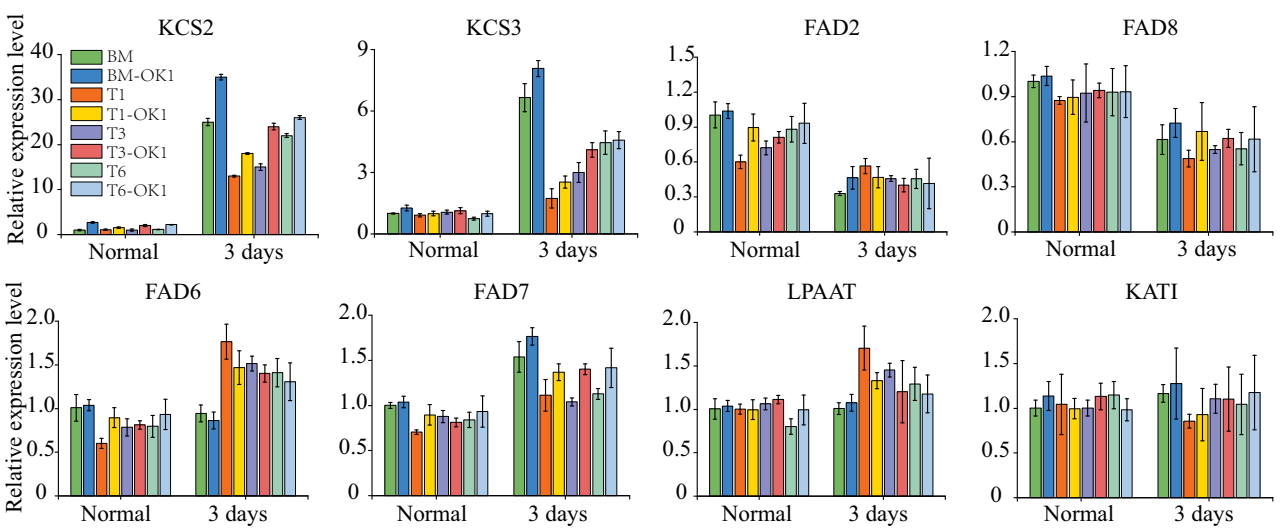

Figure 6. Real-time polymerase chain reaction analysis of the fatty acid biosynthesis genes (*KCS2*, *KCS3*, *FAD2*, *FAD6*, *FAD7*, *FAD8*, *LPAAT* and *KAT1*) in BM, BM-OK1, T1, T1-OK1, T3, T3-OK1, T6, and T6-OK1 plants grown under chilling conditions.

show that higher levels of VLCFA were correlated with lower membrane leakage and F_v/F_m reduction, suggesting that overexpression of *KCS1* could improve F_v/F_m by enhancing VLCFAs contents, thereby increasing the plant resistance against chilling condition. Similar to the F_v/F_m results, overexpression of *AKR2A* or *KCS1* resulted in increased chlorophyll content, and the chlorophyll content in co-overexpression *AKR2A* and *KCS1* lines was higher than the expression of *AKR2A* or *KCS1* alone (Figure 8c).

MDA activity results also showed that the chilling tolerance was significantly increased by co-overexpression of *AKR2A* and *KCS1* in *Arabidopsis* (Figure 8d). The results of the chlorophyll contents, anthocyanin contents, SOD activity, proline content, stomatal conductance, and transpiration rate are consistent with the MDA content results (Figure S3), indicating that the chilling tolerance of co-overexpression *AKR2A* and *KCS1* (OA/OK1) lines was greater than in plants overexpressing *AKR2A* (OA) or *KCS1* (OK1) alone. Meanwhile, the real-time PCR results show that the expression levels of fatty acid genes and cold related genes were increased in OA, OK1, and OA/OK1, indicating that overexpression of *KCS1* could increase the expression level of these genes (Figure 9 and Figure S4).

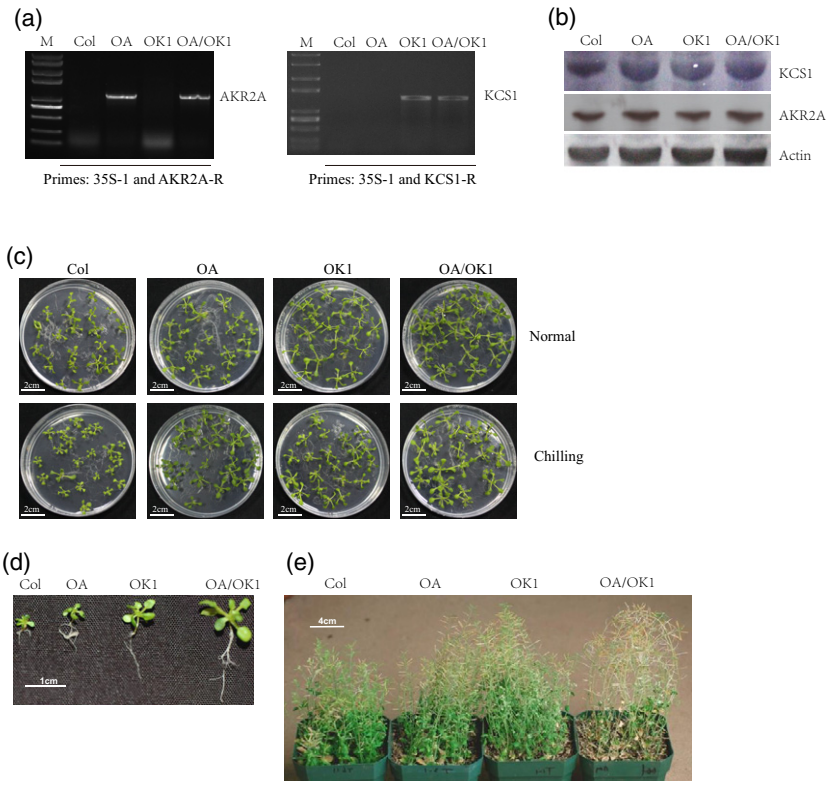

Figure 7. Co-expression of *AKR2A* and *KCS1* enhance chilling tolerance.
(a) Identification of selected transgenic lines by polymerase chain reaction and
(b) western blotting. (c, d, e) Performance of the wild-type (Col), *AKR2A* overexpression line (OA), *KCS1* expression line (OK1), and *AKR2A* and *KCS1* double overexpression line (OA/OK1) under normal or chilling conditions.

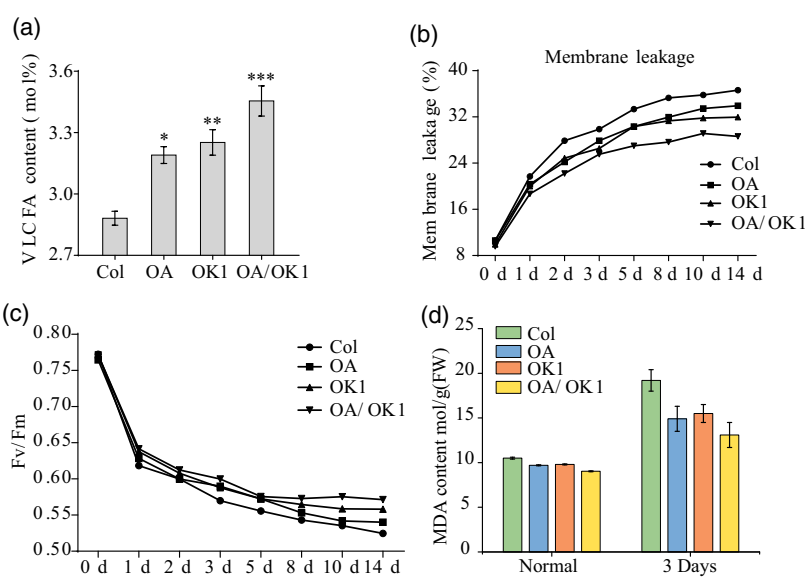

Figure 8. (a) Very long-chain fatty acids (VLCFAs) contents of Col, OA, OK1, and OA/OK1. An asterisk (*) indicates that the mean value is significantly different from that of Col: $*P < 0.05$; $**P < 0.01$.
(b) Membrane leakage (%) in Col, OA, OK1, and OA/OK1 plants.
(c) Average F_v/F_m values in response to chilling stress. (d) Malondialdehyde (MDA) content in Col, OA, OK1, and OA/OK1 plants grown under normal and chilling stress conditions.

Phenotypes of *AKR2A*-RNAi and *KCS1* knockout plants

AKR2A RNA interference and *KCS1* knockout double mutant plants (Ai/*kcs1*) were confirmed by western blotting (Figure 10a). *AKR2A*-RNAi plants (Ai) also displayed smaller physical size and curly leaf phenotypes, similar to the *akr2a*-TILLING mutants (Figure 10b,c). However, when these RNAi plants were crossed with *kcs1* mutants, the phenotypes were even more severe, with small, curled and chlorotic leaves. VLCFAs contents were lowest in double mutants and highest in wild-type plants, which indicates the chilling sensitive phenotypes of double mutants (Figure 11a). The highest membrane leakage was found to be in double mutants, whereas it was lowest in wild-type plants (Figure 11b). Consistent with the previous results, F_v/F_m is negatively correlated with the electrolyte leakage in membrane. F_v/F_m was lowest in double mutants and highest in wild-type plants (Figure 11c). MDA is considered

as a biomarker of oxidative stress and it was found that the MDA content was higher in both single and double mutants as compared to wild-type plants which indicates the chilling sensitiveness of both *AKR2A*i and *kcs1* mutants (Figure 11d). The results for chlorophyll contents, anthocyanin contents, SOD activity, proline content, stomatal conductance, and transpiration rate show that the chilling tolerance was reduced in both single and double mutants (Figure S5). Meanwhile, the expression of fatty acid biosynthesis genes and cold-related genes was reduced in both *kcs1* knockout and *akr2a* knockdown mutants, suggesting that AKR2A and KCS1 play important roles in the chilling response in Arabidopsis (Figure 12 and Figure S6).

DISCUSSION

Cold, comprising one of the major abiotic stresses, can result in plant growth disorders, low productivity, and even plant death (Lee *et al.*, 2003; Saibo *et al.*, 2009). Modification of the lipid components of membranes plays a crucial role in maintenance of cell activities when exposed to chilling stress (Somerville and Browse, 1996; Iba, 2002). Chilling tolerant plants have a high unsaturated fatty acid ratio compared to chilling sensitive plants (Dominguez *et al.*, 2010), with the major difference being the accumulation of the most highly unsaturated fatty acid, C18:3. The fatty acid composition results showed that the C18:3 content was not reduced in *akr2a* mutants, indicating that unsaturated fatty acids are not the primary reason for the reduction in the chilling tolerance capability of the *akr2a* mutants. Conversely, the chilling tolerance of *akr2a* mutants was improved by increasing VLCFAs contents via overexpression of *KCS1*. This result suggested that VLCFAs play an important role in the chilling response process in *akr2a* mutants.

Fatty acids with chain lengths of 20 or more carbons are referred to as VLCFAs (Joubès *et al.*, 2008). VLCFAs are biosynthesized by the fatty acid elongase complex in the endoplasmic reticulum (Bach and Faure, 2010). The fatty acid elongase complex in plants comprises of four enzymes: ketoacyl-CoA synthase (KCS), ketoacyl-CoA reductase (KCR), 3-hydroxy acyl-CoA dehydratase (HCD), and enoyl-CoA reductase (ECR) (Zheng *et al.*, 2005; Joubes *et al.*, 2008; Beaudoin *et al.*, 2009). In animals, VLCFAs and their derivatives participate in the animal cell differentiation and apoptosis (Hannun and Obeid, 2008; Young *et al.*, 2013). In plants, VLCFAs are important components of protective barriers or cell membranes, mediate developmental processes that are involved in biotic and abiotic responses, affect programmed cell death during plant–pathogen interactions, promote cell elongation by activating ethylene biosynthesis, and also act as signaling molecules to mediate various biological processes (Bach and Faure, 2010). VLCFAs and their derivatives are the main components of cuticular waxes, which play important roles in limiting non-stomatal water loss, protecting the plant from UV radiation, defending against pathogens, and preventing inappropriate organ fusion during development (Hall and Jones, 1961; Jenks *et al.*, 1994; Kerstiens, 2006; Yeats and Rose, 2013). Our results showed that VLCFA deficiency could affect the chilling tolerance of *Arabidopsis*.

Arabidopsis possesses 21 KCS enzymes, and different KCS genes vary in their tissue expression patterns and show distinct substrate specificities (Joubes *et al.*, 2008). KCS1 produces saturated and unsaturated VLCFAs with chain lengths of up to 22 carbon atoms (Tresch *et al.*, 2012). Real-time PCR results showed that the transcription of the KCS genes was not affected in *akr2a* mutants. By contrast, the results of western blotting show that the KCS1 expression level was reduced in *akr2a* mutants. These results suggest that AKR2A mediates KCS1 expression at the protein level. As an important molecular

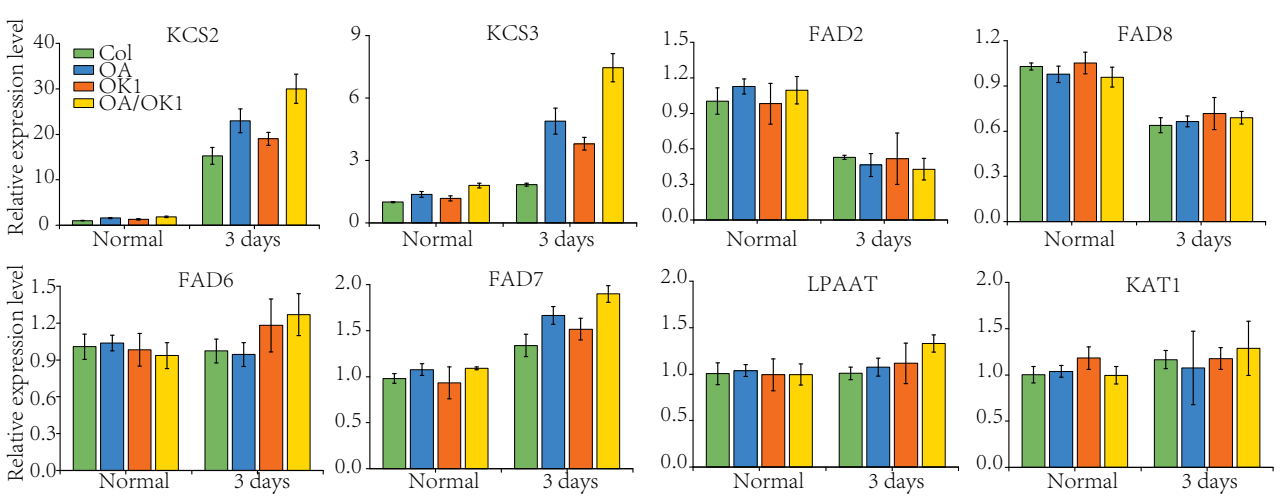

Figure 9. Real-time polymerase chain reaction analysis of the fatty acid biosynthesis gene expression in Col, OA, OK1 and, OA/OK1 under chilling stress conditions.

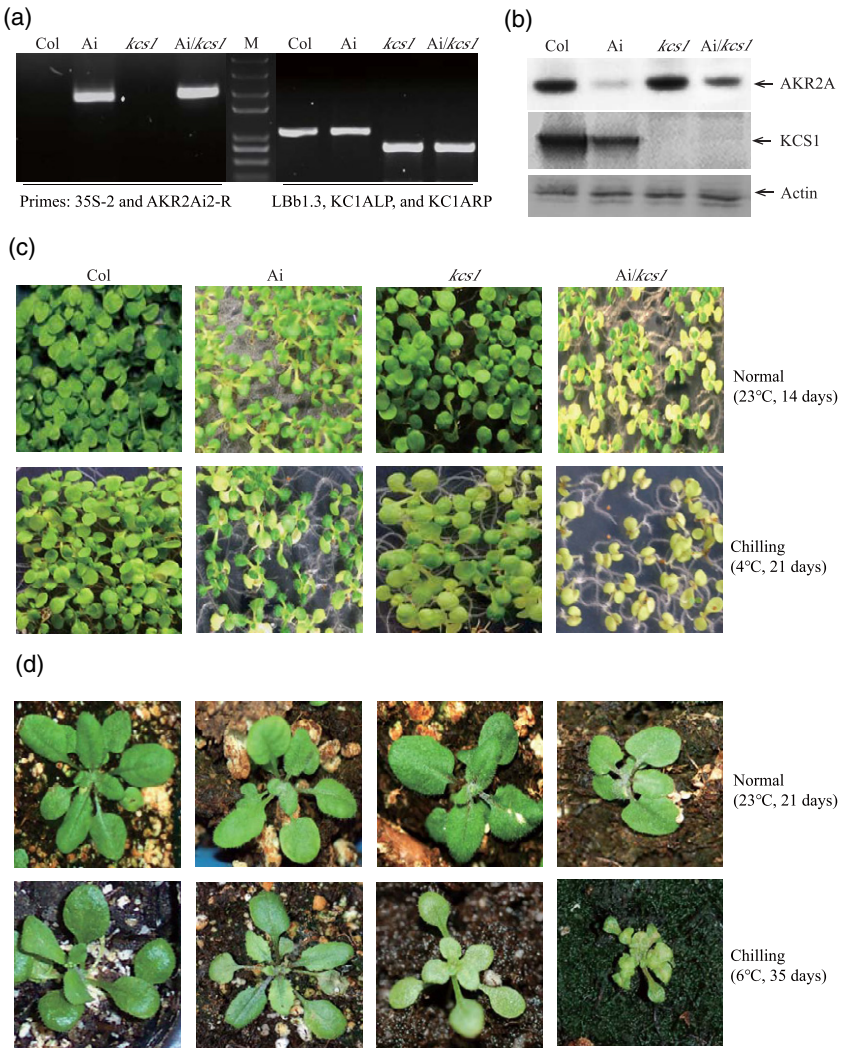

Figure 10. *AKR2A* RNA interference and *KCS1* knockout reduce plants chilling tolerance.
(a) Identification of selected transgenic lines by a polymerase chain reaction; the primers used are indicated underneath.
(b) The transgenic lines were further identified by western blotting.
(c, d) Performance of the wild-type (Col), *AKR2A* RNAi line (Ai), *KCS1* knockout line (*kcs1*), and *AKR2A* RNAi (Ai) and *KCS1* knockout double mutant line (Ai/*kcs1*) under normal or chilling conditions.

chaperone, AKR2A binds to the AKR2A binding sequence of target proteins and helps to transport these proteins to their correct destinations. Mutations in AKR2A could result in the misguidance of the target protein and ultimately protein degradation (Figure 5). Overexpressing *KCS1* in *akr2a* mutants could not increase VLCFAs contents to the same level as that in the wild-type, indicating that the expression of the other KCS proteins was also affected. As a molecular chaperone, AKR2A interacts with KCS-family proteins, and the KCS-family proteins could be affected in the *akr2a* mutants. AKR2A efficiently transports target proteins to their destinations and also promotes the stability of target proteins.

The function of polyunsaturated fatty acids in a plant's chilling tolerance has been well established in past decades. However, the role of VLCFAs ($C \geq 20$) in cold tolerance remains unclear. The molecular chaperone AKR2A was found to play an important role in plant responses to chilling stress in our previous study. A key enzyme in the VLCFAs biosynthesis pathway, KCS1 is responsible for the chilling sensitivity of *akr2a* mutants in the present study, and co-overexpressing *AKR2A* and *KCS1* significantly increased VLCFAs contents and chilling tolerance, indicating that VLCFAs play important roles in plant chilling stress. The overexpression of *KCS1* in *akr2a* mutants could not fully rescue their chilling tolerance. There might be two reasons for this observation. As a molecular chaperone, AKR2A interacts with all members of the KCS family and increasing the expression of *KCS1* could not fully compensate for the defects associated

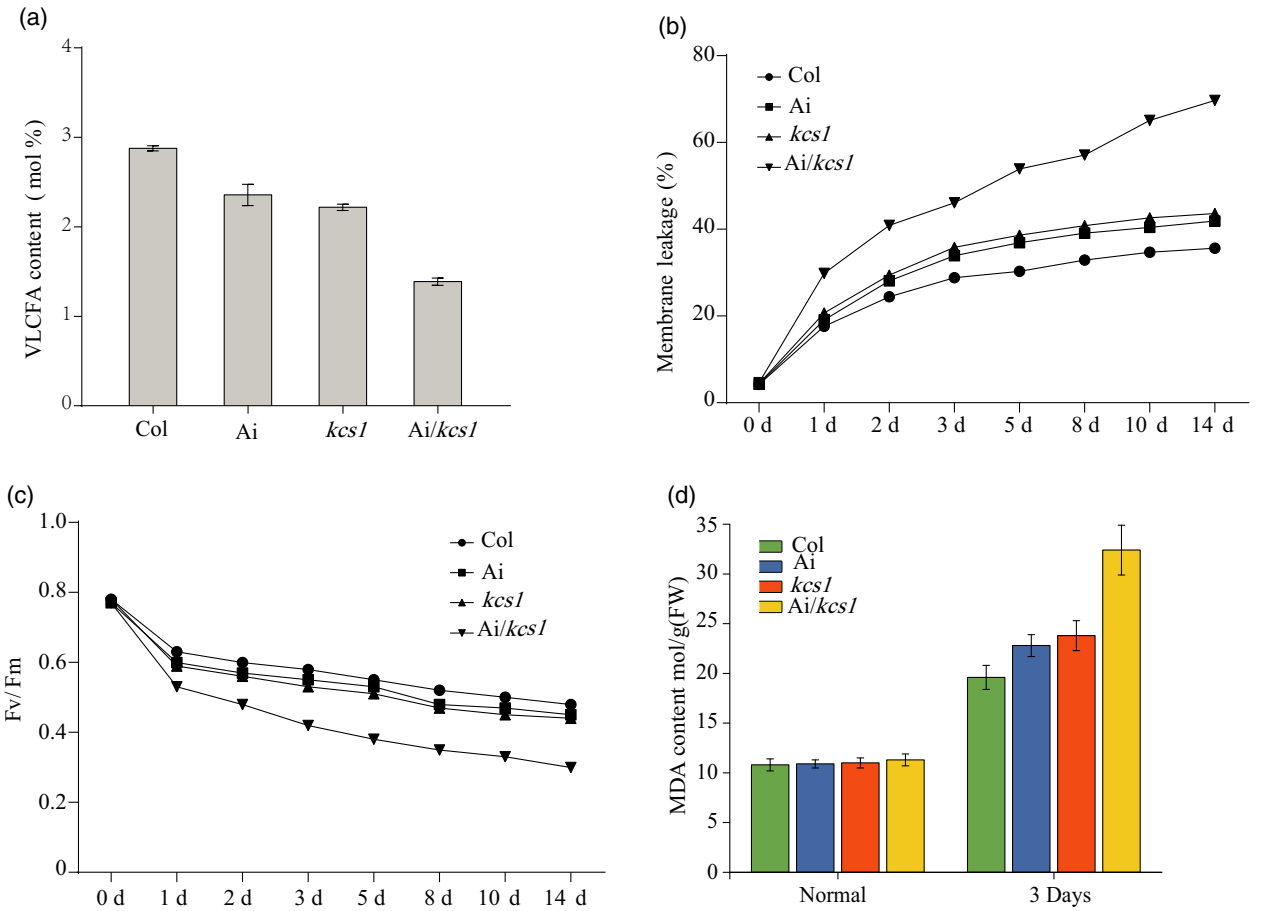

Figure 11. (a) Very long-chain fatty acids (VLCFAs) contents of Col, Ai, *kcs1* mutants, and Ai/*kcs1* double mutants.
(b) Membrane leakage (%) in Col, Ai, *kcs1* mutants, and Ai/*kcs1* double mutants.
(c) Average F_v/F_m values for Col, Ai, *kcs1* mutants, and Ai/*kcs1* double mutants in response to chilling stress.
(d) Malondialdehyde (MDA) content in Col, Ai, *kcs1* mutants, and Ai/*kcs1* double mutant plants grown under normal and chilling stress conditions.

with the other 20 KCS members. On the other hand, the chilling tolerance defects of the *akr2a* mutants were caused by the point-mutation in *AKR2A*. A previous study demonstrated that overexpressing *AKR2A* in *akr2a* mutants could fully rescue the chilling tolerance (Shen *et al.*, 2010). The defect of KCS1 localization to the endoplasmic reticulum remained in the *KCS1*-overexpressing *akr2a* plants. Thus, overexpression of *KCS1* could increase the potential for KCS1 to bind to the endoplasmic reticulum in other ways.

The CBF pathway has a prominent role in cold acclimation, and the CBF gene family can be transiently induced by low temperature, leading to the activation of downstream genes. The CBF binding sequence was detected in both *AKR2A* and *KCS1* promoter sequences, and real-time PCR results showed that the expression of both *AKR2A* and *KCS1* was decreased 24 h post-chilling treatment, and then expression was notably increased. However, the expression of CBF1 and CBF2 was activated at 0.5 h under chilling. These results indicate that the expression of *AKR2A* and *KCS1* was increased by CBF under chilling treatment (Figure S7). Our results show that AKR2A plays an important role in VLCFA synthesis by mediating KCS1 expression (Figure 13). Overexpressing *KCS1* could increase VLCFAs contents, which reduces membrane leakage by maintaining the membrane stability. Membrane stability is positively associated with the photosynthetic rate (Gombos *et al.*, 1994), and the high VLCFAs contents could enhance the photosynthetic rate in plants under chilling conditions (Figure 11).

EXPERIMENTAL PROCEDURES

Plant materials

KCS1 T-DNA insertion and *akr2a*-TILLING lines were ordered from the *Arabidopsis* Biological Resource Center (Columbus, OH, USA). *Arabidopsis thaliana* Col and Col er105 (BM) were used as the wild-type. Seeds were grown in 1/2 MS media or in peat moss-enriched soil in a chamber under long-day conditions (14 :10 h light/dark photocycle, 24°C day/23°C night, 65% humidity and a light intensity of 12 000 lux).

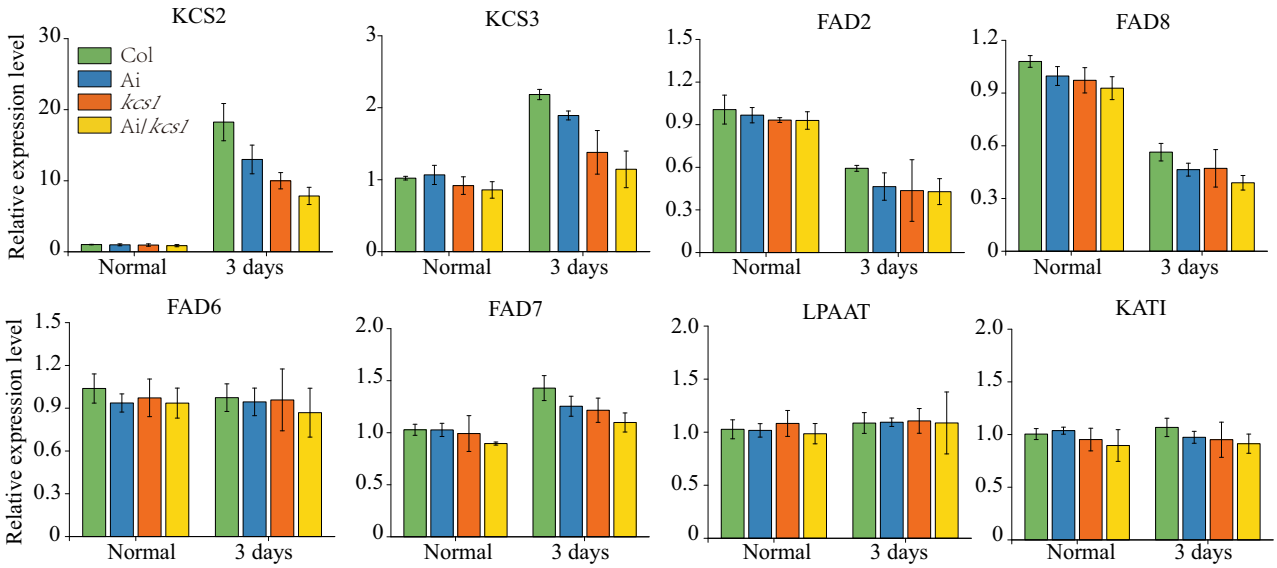

Figure 12. Real-time polymerase chain reaction analysis of the fatty acid biosynthesis gene expression in Col, Ai, *kcs1* mutants, and Ai/*kcs1* double mutants.

Generation of plants overexpressing *AKR2A* and *KCS1*

The *KCS1* (AT1G01120) coding sequence was PCR amplified using the primer pair KCS1-F and KCS1-R, and then subcloned into pGWB17 (Jefferson *et al.*, 1987). The recombinant constructs were transformed into *Agrobacterium tumefaciens* GV3101 and confirmed by PCR. The correct transformation vector was introduced into wild-type and various plants via the floral dip method of Clough and Bent (1998). Positive transgenic lines were screened on hygromycin plates and identified by PCR. The transgenic lines were selfed for two generations before screening for homozygous lines. For the construction of *AKR2A* (AT4G35450) overexpressing plants, *AKR2A* was PCR amplified with primer pair AKR2A-F and AKR2A-R, and then subcloned into pBI121 (Jefferson *et al.*, 1987). The recombinant construct was transformed into GV3101 and then was introduced into wild-type to generate the *AKR2A* overexpressing plants. The transgenic lines were selfed for two generations before screening for homozygous lines.

For generating plants co-overexpressing *AKR2A* and *KCS1*, the *AKR2A* and *KCS1* overexpressing homozygous line were sexually hybridized. The hybrid seeds were screened on hygromycin and kanamycin containing 1/2 MS media.

Generation of *AKR2A* RNAi (Ai) and Ai/*kcs1*

For the construction of *AKR2A* interference (RNAi) plants, part of *AKR2A* (850 bp) was PCR amplified with the primer pair AKR2Ai1-F and AKR2Ai1-R, and the reverse sequence was amplified by AKR2Ai2-F and AKR2Ai2-R, and then subcloned into pFGC5941 (Jefferson *et al.*, 1987). The recombinant plasmid was transformed into GV3101 and then was introduced into wild-type to generate the *AKR2A* interference plants (Ai). The transgenic lines were selfed for two generations before screening for homozygous lines.

For generating plants with *AKR2A* interference and *kcs1*, the Ai and *kcs1* homozygous line was sexually hybridized. The hybrid seeds were screened on 1/2 MS media containing phosphinothricin and kanamycin.

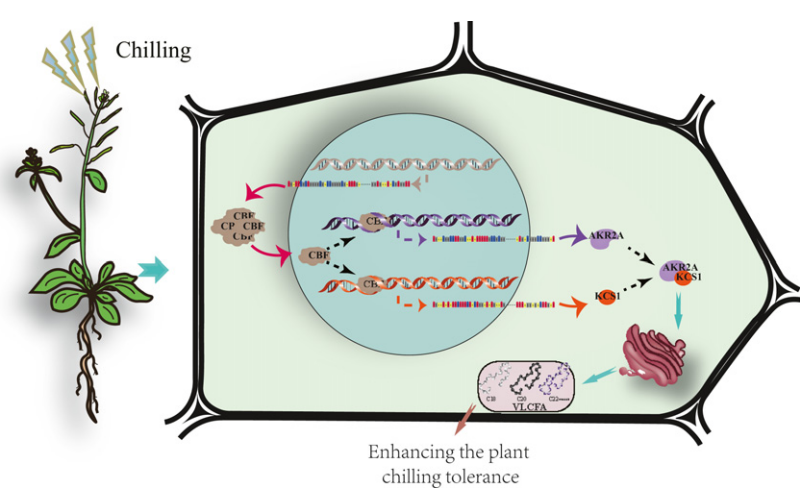

Figure 13. A proposed model for AKR2A and KCS1 to enhance chilling tolerance in Arabidopsis plants.

Histochemical GUS assays

The *AKR2A* promoter was PCR amplified from the genomic DNA of *Arabidopsis* using the primers AKR2A-proF and AKR2A-proR. A 1535-bp fragment was amplified and then cloned into pBI121. The successful construct was transformed into GV3101 and verified by PCR. The construct was then transformed into *Arabidopsis*. The transgenic lines were selfed for two generations before screening for homozygous lines. The homozygous lines were grown under normal or chilling conditions, and the tissues were collected at different time intervals of their developmental stages. The wild-type was used as the negative control. GUS assays were performed as described by Beeckmans *et al.* (1994). Samples mounted in lactic acid were observed and photographed with a stereomicroscope (Leica, Wetzlar, Germany).

Real-time PCR analysis

Total RNA was extracted from the treated seedlings using the RNAprep Pure Plant kit (Tiangen, Beijing, China), and the RNA samples were treated with DNAase I. The complementary DNA (cDNA) synthesis was performed in accordance with the manufacturer's instructions using the Quantscript RT Kit (Tiangen). A real-time PCR (RT-PCR) was performed on an ABI StepOne Plus system using the SYBR Green PCR Master Mix kit (Applied Biosystems, Foster City, CA, USA). Oligonucleotides for real-time PCR primers are listed in Table S1. Relative gene expression levels were determined using the $2^{-\Delta\Delta CT}$ method (Livak and Schmittgen, 2001). All experimental samples were assayed in triplicates. The *actin8* mRNAs in each sample was determined and used to normalize for differences in total RNA amounts.

Chilling tolerance assays

For the chilling tolerance assay, seeds were grown in 1/2 MS media for 7 days at 23°C under long-day conditions, and then they were moved into a 4°C growth chamber under long-day conditions (16:8 h) for 14 days. Finally, the plants were photographed.

For seedlings in soil, the 10-day-old plants were transferred to 6°C under a 16:8 h photocycle for 60 days, and then the chilling-treated plants were moved to 23°C for 7 days.

Electrolyte leakage determination

To determine membrane electrolyte leakage, the aerial parts of plants grown on MS plates were collected after chilling treatment and electrolytes were measured using a method described previously (Hong *et al.*, 2003). Briefly, 1.0 g of samples were rinsed with deionized water and shaken for 1 h at 22°C. Conductivity was measured using an electrical conductivity meter (SG23; Mettler Toledo, Shanghai, China) as ELn and the total conductivity (ELb) was measured after the plants were boiled for 10 min. Then membrane electrolyte leakage was calculated as a percentage of membrane leakage (%) = ELn/ELb × 100.

Chlorophyll fluorescence analysis and chlorophyll measurement

Chlorophyll fluorescence was measured using a mini-PAM system (MAXI; Heinz Walz, Effeltrich, Germany). Fully expanded leaves were used for the experiment. The seedlings were stored in the dark for 8 h before the measurements were taken. The F_v/F_m of chlorophyll fluorescence parameter was measured and calculated in accordance with a previous method (van Kooten and Snel, 1990). $F_v/F_m = (F_m - F_o)/F_m$.

To estimate the total chlorophyll content, approximately 0.1 g of fresh rosette leaves were ground in liquid nitrogen. Chlorophyll was extracted from leaf tissues with 80% ice-cold ethanol and transferred to darkness for the indicated time. The extracts were centrifuged at 16 000 ***g*** for 10 min at 4°C, and the absorbance readings at 645 and 663 nm were determined using an UV-visible spectrophotometer. The chlorophyll content was calculated in accordance with a method described previously (Lichtenthaler, 1987).

Yeast-2-hybrid assays

To map the interaction domains, AKR2A was used as bait and KCS1 was used as prey in the AKR2A–KCS1 interaction assay. A series of AKR2A and KCS1 fusion constructs were made using the bait vector pPR3-N and pBT-STE (Dualsystem Biotech, Schlieren, Switzerland). Yeast cells and library screening were conducted in accordance with the manufacturer's instructions. After crossing, the cells were plated onto a selective medium to select resistant clones. Potential interactions were confirmed on a more selective medium to increase the stringency of the screening.

For the yeast-2-hybrid library screening assay, AKR2A was used as bait and cloned to the vector pEG202. The Arabidopsis library cloned in prey vector pJG4-5, and the screening of the yeast-1-hybrid library was performed as described previously (Shen *et al.*, 2010).

MDA assay

Fresh rosette leaves (0.1 g) were added to 3 ml of 10% (w/v) trichloroacetic acid, ground into a slurry, and incubated at 4°C for 12 h, after which an additional 9 ml of 10% trichloroacetic acid was added. The homogenate was centrifuged at 2800 ***g*** for 5 min. A total of 2 ml of 0.6% (w/v) thiobarbituric acid was added to 2 ml supernatant. The mixtures were incubated in a 100°C waterbath for 15 min and then quickly cooled in ice. The absorbance of the supernatant at 600, 532, and 450 nm was measured after centrifugation at 2800 ***g*** for 5 min. The MDA level was calculated using the absorption coefficient: MDA (mmol g^{-1} FW) = $[6.45 \times (A_{532} - A_{600}) - 0.56 \times A_{450}] \times V_t/V_m \times W$, where V_t is the total volume of extraction liquid in the current experiment (V_t = 10 ml); V_m is the volume used for measurement in this experiment (V_0 = 2.0 ml); W is the sample fresh weight (W = 0.1 g). This experiment was repeated three times per line.

BiFC assay

For BiFC analysis, the interacting region of *AKR2A* and *KCS1* was cloned into pCambia-split yellow fluorescent protein (YFP) vector. These vectors were transformed into the *Agrobacterium* strains GV3101. Equal volumes of different *Agrobacterium* suspensions carrying pCambia-AKR2A-CYFP, KCS1-NYFP, p19 were mixed. The re-suspended cells were infiltrated into leaves of tobacco plants as described previously. The fluorescence signals in infiltrated leaves were analyzed via confocal microscopy (TCS SP5; Leica).

Co-immunoprecipitation assay

Total protein extracts (500 μg) were incubated with 10 μg of AKR2A antibodies (Yan *et al.*, 2002), then 50 μl of washed protein A-agarose slurry at 4°C was added, and the mixture was incubated on a rotator for 8 h. The agarose-immune complexes were spun down at 6000 ***g*** for 30 s at 4°C and washed five times in wash buffer [125 mM Tris-Cl, 2% sodium dodecyl sulphate (SDS), 20% glycerol, 200 mM dithiothreitol, 0.01% bromophenol blue, and 0.1% NP-40, pH 6.8]. The samples were boiled for 5 min,

centrifuged at 6000 ***g*** for 30 sec to remove protein A-agarose beads, and then subjected to immunoblot analyses with the appropriate antibodies.

Western blotting

Seedlings were ground in liquid nitrogen and homogenized in a protein extraction buffer (150 mM NaCl, 50 mM Tris-Cl, and 5 mM ethylenediaminetetraacetic acid, pH 7.6). Cell debris were removed by centrifugation at 16 000 ***g*** for 15 min at 4°C. For western blot analysis, the supernatants were denatured with 5 × SDS loading buffer (Tiangen) and separated on 10 % SDS-polyacrylamide gel. The separated proteins were transferred to a polyvinylidene fluoride membrane (Millipore, Bedford, MA, USA). To detect AKR2A and KCS1, the membrane was incubated with rabbit polyclonal anti-AKR2A or anti-KCS1 antibodies, respectively in TBS buffer (Sangon, Shanghai, China) containing 0.05% Tween-20. For actin detection, the membrane was incubated with mouse monoclonal anti-actin antibodies (Sigma, St Louis, MO, USA). Bands were visualized with BCIP/NBT Alkaline Phosphatase Color Development Kit (Beyotime, Nanjing, China), in accordance with the manufacturer's instructions.

Fatty acid methyl ester analysis

All of the experiments were performed with three biological repeats. The total lipid was extracted from the ground seeds and lipid content was analyzed as described by (Sukhija and Palmquist, 1990); the fatty acid composition was analyzed using gas chromatography (Hewlett-Packard, Palo Alto, CA, USA). In the present study, the long-chain saturated acids include C20:0, C22:0, and C24:0; the saturated fatty acids include C14:0, C16:0, C18:0, C20:0, C22:0, and C24:0; and the unsaturated fatty acids include C16:1, C18:1, C18:2, and C18:3. The content of each fatty acid was expressed as the percentage of total fatty acids.

ACKNOWLEDGEMENTS

This project was supported by the Key Technologies R & D Program for Crop Breeding of Zhejiang Province (2016C02054-19), the National Key R&D Program for Crop Breeding (2016YFD0100306-4), the Natural Science Foundation of China (31771846 and 31670303), Zhejiang Provincial Natural Science Foundation of China (LY17C020006 and LY18C020005), State Key Laboratory for Quality and Safety of Agro-products of China (2010DS700124-ZZ1904), and the Joint Laboratory of Olive Oil Quality and Nutrition among China, Australia, and Spain.

CONFLICT OF INTERESTS

The authors declare that they have no conflicts of interest.

AUTHOR CONTRIBUTIONS

LC and GXS designed the experiments and the research plan. LC, WJH, NM, YFC, HLL, and YQH performed the experiments. NM, LC, QXY, JW, WCL, SFY, and HZ analyzed the data and wrote the article.

SUPPORTING INFORMATION

Additional Supporting Information may be found in the online version of this article.

Figure S1. Overexpression of *KCS1* enhances the chilling tolerance of BM and *akr2a* mutants.

Figure S2. RT-PCR analysis of genes for BM and *akr2a* mutants under normal and chilling conditions.

Figure S3. Analysis of chlorophyll, anthocyanins, proline, SOD activity, transpiration rate in Col-0, overexpressing *AKR2A* and *KCS1* plants under normal and chilling conditions.

Figure S4. RT-PCR analysis of genes in Col-0, overexpressing *AKR2A* and *KCS1* plants under normal and chilling conditions.

Figure S5. Analysis of chlorophyll, anthocyanins, proline, SOD activity, transpiration rate in Col-0, AKR2Ai and *kcs1* mutant plants under normal and chilling conditions.

Figure S6. RT-PCR analysis of genes in Col-0, AKR2Ai and *kcs1* mutant plants under normal and chilling conditions.

Figure S7. Analysis of *KCS1* promoter sequence.

Figure S8. RT-PCR analysis of *AKR2A*, *KCS1*, *CBF1* and *CBF2* genes in BM and akr2a mutants under normal and chilling conditions.

Table S1. Primer sequence.

Data S1. Supplemental Methods.

REFERENCES

Bach, L. and Faure, J.D. (2010) Role of very-long-chain fatty acids in plant development, when chain length does matter. *C.R. Biol.* **333**, 361–370.

Bach, L., Michaelson, L.V., Haslam, R. *et al.* (2008) The very-long-chain hydroxy fatty acyl-CoA dehydratase PASTICCINO2 is essential and limiting for plant development. *Proc. Natl Acad. Sci. USA*, **105**, 14727–14731.

Beaudoin, F., Wu, X., Li, F., Haslam, R.P., Markham, J.E., Zheng, H., Napier, J.A. and Kunst, L. (2009) Functional characterization of the Arabidopsis beta-ketoacyl-coenzyme A reductase candidates of the fatty acid elongase. *Plant Physiol.* **150**, 1174–1191.

Beeckmans, S., Khan, A.S., Kanarek, L. and Van Driessche, E. (1994) Ligand binding on to maize (Zea mays) malate synthase: a structural study. *Biochem. J.* **303**, 413–421.

Chen, M. and Thelen, J.J. (2013) ACYL-LIPID DESATURASE2 is required for chilling and freezing tolerance in Arabidopsis. *Plant Cell*, **25**, 1430–1444.

Chinnusamy, V., Zhu, J.K. and Sunkar, R. (2010) Gene regulation during cold stress acclimation in plants. *Methods Mol. Biol.* **639**, 39–55.

Clough, S.J. and Bent, A.F. (1998) Floral dip: a simplified method for Agrobacterium-mediated transformation of *Arabidopsis thaliana*. *Plant J.* **16**, 735–743.

Dominguez, T., Hernandez, M.L., Pennycooke, J.C., Jimenez, P., Martinez-Rivas, J.M., Sanz, C., Stockinger, E.J., Sanchez-Serrano, J.J. and Sanmartin, M. (2010) Increasing omega-3 desaturase expression in tomato results in altered aroma profile and enhanced resistance to cold stress. *Plant Physiol.* **153**, 655–665.

Fehling, E. and Mukherjee, K.D. (1991) Acyl-CoA elongase from a higher plant (Lunaria annua): metabolic intermediates of very-long-chain acyl-CoA products and substrate specificity. *Biochem. Biophys. Acta*, **1082**, 239–246.

Gombos, Z., Wada, H. and Murata, N. (1994) The recovery of photosynthesis from low-temperature photoinhibition is accelerated by the unsaturation of membrane lipids: a mechanism of chilling tolerance. *Proc. Natl Acad. Sci. USA*, **91**, 8787–8791.

Graham, D. and Patterson, B.D. (1982) Responses of plants to low, nonfreezing temperatures: proteins, metabolism, and acclimation. *Annu. Rev. Plant Physiol.* **33**, 347–372.

Hall, D.M. and Jones, R.I. (1961) Physiological significance of surface wax on leaves. *Nature*, **191**, 95–96.

Hannun, Y.A. and Obeid, L.M. (2008) Principles of bioactive lipid signalling: lessons from sphingolipids. *Nat. Rev. Mol. Cell Biol.* **9**, 139–150.

Hong, S.W., Lee, U. and Vierling, E. (2003) Arabidopsis hot mutants define multiple functions required for acclimation to high temperatures. *Plant Physiol.* **132**, 757–767.

Hong, Z., Xiao, L. and Shen, G. (2010) Is AKR2A an essential molecular chaperone for a class of membrane-bound proteins in plants? *Plant Signal. Behav.* **5**(11), 1520–1522.

Iba, K. (2002) Acclimative response to temperature stress in higher plants: approaches of gene engineering for temperature tolerance. *Annu. Rev. Plant Biol.* **53**, 225–245.

Jefferson, R.A., Kavanagh, T.A. and Bevan, M.W. (1987) GUS fusions: beta-glucuronidase as a sensitive and versatile gene fusion marker in higher plants. *EMBO J.* **6**, 3901–3907.

Jenks, M.A., Joly, R.J., Peters, P.J., Rich, P.J., Axtell, J.D. and Ashworth, E.N. (1994) Chemically induced cuticle mutation affecting epidermal conductance to water vapor and disease susceptibility in Sorghum bicolor (L.) Moench. *Plant Physiol.* **105**, 1239–1245.

Joubes, J., Raffaele, S., Bourdenx, B., Garcia, C., Laroche-Traineau, J., Moreau, P., Domergue, F. and Lessire, R. (2008) The VLCFA elongase gene family in Arabidopsis thaliana: phylogenetic analysis, 3D modelling and expression profiling. *Plant Mol. Biol.* **67**, 547–566.

Joubès, J., Raffaele, S., Bourdenx, B., Garcia, C., Laroche-Traineau, J., Moreau, P., Domergue, F. and Lessire, R. (2008) The VLCFA elongase gene family in Arabidopsis thaliana: phylogenetic analysis, 3D modelling and expression profiling. *Plant Mol. Biol.* **67**, 547–566.

Jr, B.J. and Sprecher, H. (1977) An analysis of partial reactions in the overall chain elongation of saturated and unsaturated fatty acids by rat liver microsomes. *J. Biol. Chem.* **252**, 6736–6744.

Jr, B.J. and Sprecher, H. (1979) The isolation of acyl-CoA derivatives as products of partial reactions in the microsomal chain elongation of fatty acids. *Biochem. Biophys. Acta*, **573**, 436.

Kerstiens, G. (2006) Water transport in plant cuticles: an update. *J. Exp. Bot.* **57**, 2493–2499.

Lee, S.E., Hwang, H.J., Ha, J.S., Jeong, H.S. and Kim, J.H. (2003) Screening of medicinal plant extracts for antioxidant activity. *Life Sci.* **73**, 167–179.

Lichtenthaler, H.K. (1987) Chlorophylls and carotenoids: pigments of photosynthetic biomembranes. *Methods Enzymol.* **148C**, 350–382.

Livak, K.J. and Schmittgen, T.D. (2001) Analysis of relative gene expression data using real-time quantitative PCR and the 2(-Delta Delta C(T)) Method. *Methods*, **25**, 402–408.

Millar, A.A. and Kunst, L. (1997) Very-long-chain fatty acid biosynthesis is controlled through the expression and specificity of the condensing enzyme. *Plant J.* **12**, 121–131.

Nobusawa, T. and Umeda, M. (2012) Very-long-chain fatty acids have an essential role in plastid division by controlling Z-ring formation in Arabidopsis thaliana. *Genes Cells*, **17**, 709–719.

Nugteren, D.H. (1965) The enzymic chain elongation of fatty acids by rat-liver microsomes. *Biochem. Biophys. Acta*, **106**, 280–290.

Palta, J.P., Whitaker, B.D. and Weiss, L.S. (1993) Plasma membrane lipids associated with genetic variability in freezing tolerance and cold acclimation of Solanum Species. *Plant Physiol.* **103**, 793–803.

Saibo, N.J., Lourenco, T. and Oliveira, M.M. (2009) Transcription factors and regulation of photosynthetic and related metabolism under environmental stresses. *Ann. Bot.* **103**, 609–623.

Shen, G., Kuppu, S., Venkataramani, S., Wang, J., Yan, J., Qiu, X. and Zhang, H. (2010) ANKYRIN REPEAT-CONTAINING PROTEIN 2A is an essential molecular chaperone for peroxisomal membrane-bound ASCORBATE PEROXIDASE3 in Arabidopsis. *Plant Cell*, **22**, 811–831.

Smirnova, A., Leide, J. and Riederer, M. (2013) Deficiency in a very-long-chain fatty acid β-ketoacyl-coenzyme a synthase of tomato impairs microgametogenesis and causes floral organ fusion. *Plant Physiol.* **161**, 196–209.

Somerville, C. and Browse, J. (1996) Dissecting desaturation: plants prove advantageous. *Trends Cell Biol.* **6**, 148–153.

Sukhija, P.S. and Palmquist, D.L. (1990) Dissociation of calcium soaps of long-chain fatty acids in rumen fluid. *J. Dairy Sci.* **73**, 1784–1787.

Todd, J., Postbeittenmiller, D. and Jaworski, J.G. (1999) KCS1 encodes a fatty acid elongase 3-ketoacyl-CoA synthase affecting wax biosynthesis in Arabidopsis thaliana. *Plant J.* **17**, 119.

Tresch, S., Heilmann, M., Christiansen, N., Looser, R. and Grossmann, K. (2012) Inhibition of saturated very-long-chain fatty acid biosynthesis by mefluidide and perfluidone, selective inhibitors of 3-ketoacyl-CoA synthases. *Phytochemistry*, **76**, 162–171.

van Kooten, O. and Snel, J.F. (1990) The use of chlorophyll fluorescence nomenclature in plant stress physiology. *Photosynth. Res.* **25**, 147–150.

Williams, J.P., Khan, M.U. and Wong, D. (1992) Low temperature-induced fatty acid desaturation in Brassica napus: thermal deactivation and reactivation of the process. *Biochem. Biophys. Acta*, **1128**, 275–279.

Yan, J., Wang, J., and Zhang, H. (2002) An ankyrin repeat-containing protein plays a role in both disease resistance and antioxidation metabolism. *Plant J.* **29**, 193–202.

Yeats, T.H. and Rose, J.K. (2013) The formation and function of plant cuticles. *Plant Physiol.* **163**, 5–20.

Young, M.M., Kester, M. and Wang, H.G. (2013) Sphingolipids: regulators of crosstalk between apoptosis and autophagy. *J. Lipid Res.* **54**, 5–19.

Zheng, H., Rowland, O. and Kunst, L. (2005) Disruptions of the Arabidopsis Enoyl-CoA reductase gene reveal an essential role for very-long-chain fatty acid synthesis in cell expansion during plant morphogenesis. *Plant Cell*, **17**, 1467–1481.